HHS Public Access

Author manuscript

Science. Author manuscript; available in PMC 2023 January 07.

Published in final edited form as:

Science. 2022 January 07; 375(6576): 86–91. doi:10.1126/science.abl4732.

Cryo-EM structure of human GPR158 receptor coupled to the RGS7-Gβ5 signaling complex

Dipak N. Patil[1,#], **Shikha Singh**[2,#], **Thibaut Laboute**[1], **Timothy S. Strutzenberg**[3], **Xingyu Qiu**[4,5], **Di Wu**[4,5], **Scott J. Novick**[3], **Carol V. Robinson**[4,5], **Patrick R. Griffin**[3], **John F. Hunt**[2], **Tina Izard**[6], **Appu K. Singh**[7,8,*], **Kirill A. Martemyanov**[1,*]

[1]Department of Neuroscience, The Scripps Research Institute, Jupiter, FL 33458, USA

[2]Department of Biological Sciences, Columbia University New York, NY 10027

[3]Department of Molecular Medicine, The Scripps Research Institute, Jupiter, FL 33458, USA

[4]Department of Chemistry, University of Oxford, 12 Mansfield Road, Oxford OX1 3TA, U.K.

[5]The Kavli Institute for Nanoscience Discovery, Oxford, OX1 3QU, UK

[6]Department of Integrative Structural and Computational Biology, The Scripps Research Institute, Jupiter, FL 33458, USA

[7]Department of Biological Sciences and Bioengineering, Indian Institute of Technology, Kanpur 208016, India

[8]Mehta Family Centre for Engineering in Medicine, Indian Institute of Technology Kanpur, Kanpur, Uttar Pradesh 208016, India

Abstract

GPR158 is an orphan G-protein-coupled receptor (GPCR) highly expressed in the brain where it controls synapse formation and function. GPR158 has also been implicated in depression, carcinogenesis and cognition. However, the structural organization and signaling mechanisms of GPR158 are largely unknown. Here, we report structures of the human GPR158 alone and bound to an RGS signaling complex, determined using single-particle cryo-electron microscopy (cryoEM). The structures reveal a homodimeric organization stabilized by a pair of phospholipids and the presence of an extracellular Cache domain, an unusual ligand-binding domain in GPCRs.-. We further demonstrate the structural basis of GPR158 coupling to RGS7-Gβ5. Together, these

[*]**Co-corresponding authors**: Dr. Kirill A. Martemyanov, kirill@scripps.edu; Dr. Appu K. Singh, singhappu@iitk.ac.in.
[#]These authors contributed equally.

Author contributions: D.N.P. and K.A.M. conceived the project; D.N.P. performed the constructs design and cloning, preliminary screening of constructs and generation of BacMam viruses, protein expression and production, protein purification for cryoEM and biophysical studies, buffer optimization and preliminary screening of samples for EM study, model building and structural analysis, mutagenesis and biochemical experiments; S.S. performed final cryoEM grids preparation; D.N.P. and S.S. EM data processing; T.L. performed functional experiments; T.S. performed cross-linking MS; S.J.N. performed HDX-MS; X.Q. and D.W. performed lipidomics; J.F.H. supervised cryoEM studies; T.I. guided biochemical protein purification experiments and sample preparation for the EM; P.R.G. supervised cross-linking MS and HDX-MS; C.V.R. supervised lipidomics studies; A.K.S. supervised cryoEM studies and built the atomic models; D.N.P. and K.A.M. wrote the manuscript with input from all other authors; K.A.M. supervised the overall project implementation.

Competing interests: Authors declare that they have no competing interests.

results provide insights into the unusual biology of orphan receptors and the formation of GPCR-RGS complexes.

G protein-coupled receptors (GPCR) form the largest family of proteins encoded in mammalian genomes that detect extracellular signals to program cellular response. They are essential to understanding physiology, disease, and drug development (1, 2). The canonical model posits that GPCRs transduce their signals by recruitment and activation of heterotrimeric G proteins (3). This model was subsequently updated to accommodate alternative signal propagation by recruitment of β-arrestin scaffolds (4). Termination of GPCR signaling requires the action of Regulator of G protein Signaling (RGS) proteins that directly deactivate G proteins (5, 6). GPCRs and RGS are thus classically considered as opposing forces in controlling cellular responses. However, they have long been reported to form complexes suggesting existence of additional signaling mechanisms (7, 8).

Orphan GPCRs are attractive drug targets with important roles in physiology and disease (9, 10). Yet, in many cases, their mechanisms, ligands, and signaling reactions are poorly understood. An example is the orphan receptor GPR158. It is one of the most abundant GPCRs in the brain, well documented for its pivotal role in regulating mood, cognition and implicated in a range of diseases (11–15). It shapes synaptic organization and function by regulating ion channels and second messengers (16, 17). GPR158 features a large extracellular domain with distinctive sequence suggesting unique ligand recognition principles. Central feature of GPR158 is its association with the neuronal RGS protein: RGS7-Gβ5 complex (11). Binding with GPR158 potentiates RGS activity (18) and both proteins act together regulating homeostasis of second messenger cAMP to control neuronal activity with significant impact on brain physiology (19). However, its signaling mechanisms and structural organization remain elusive.

We employed single-particle cryogenic electron microscopy (cryoEM) to obtain structures of GPR158 in the apo state and in complex with RGS7-Gβ5 at an average resolution of 3.4 Å and 3.3 Å, respectively (fig. S1, S2, S3 and table S1). The structure of GPR158 reveals a homodimer assembly (Fig. 1A) where the dimerization interface involves the extracellular domain, the transmembrane (TM) region, and cytoplasmic elements (Fig. 1A and fig. 4A). Each protomer features prominent extracellular and transmembrane domains linked by a flexible ‘stalk’ domain. The N-terminal portion of the extracellular domain (ECD) adopts a characteristic Cache domain fold. The TM region of protomers contains well-resolved helices. We observed continuous density for TM1 through TM7 including all extra- and intracellular loops (ECLs and ICLs), except for ICL2. We further detected two phospholipids in the cavity generated by the dimeric interface and several cholesterol-like molecules packed against hydrophobic residues of the TM domain, including the dimeric interface. The density at the ECD is limited and many of the side chain densities are not visible. The overall B-factor and average side chain B-factor for ectodomain is high (>50 Å) (fig. S4C), suggesting greater conformational flexibility of ECD. Nevertheless, the key organizational features of ECD are clearly distinguishable.

The structure of the GPR158 homodimer in complex with RGS7-Gβ5 shows that one RGS7-Gβ5 heterodimer interacts with two sites on GPR158 (Fig. 1B and fig. S4B). The

first interface is a two-helical bundle comprising a C-terminal helix (CT-CC) from each protomers. The second contact surface is at the dimer interface between 7TM regions of GPR158 protomers. We found that in RGS7 bound state, the density for the GPR158 ectodomain becomes diffuse. Although the density is observable at low contour, the model could not be built. This higher conformational flexibility at the ectodomain, possibly induced by RGS7-Gβ5 binding, suggests that extracellular and intracellular elements of the complex could be allosterically connected. This notion is further supported by the 3D variability analysis that showed that ECD undulations coincide with RGS7-Gβ5 binding (movie S1 and S2). Along with that, GPR158 CT-CC and RGS domain of RGS7 shows higher B-factor, reflecting conformational dynamics at these regions (fig. S4D). Cross-linking mass spectroscopy (XL-MS) confirmed the main contact points in the complex at the single amino acid level (fig. S5).

Detailed analysis of the 7TM domain of GPR158 reveals a compact dimeric interface (Fig. 2A and Figure S6a). Superposition of the two protomer 7TM regions shows a similar arrangement of all the elements including extra- and intracellular loops with r.m.s.d. value of 0.35 Å (fig. S6B). Within each protomer, ECL2 C573 forms a disulfide bond with TM3 C481, an interaction conserved throughout GPCRs. The β-hairpin of ECL2 interacts with the stalk-TM linker through hydrophobic interactions, bridging the ectodomain and TM domain of each protomer. ECL2 also interacts with ECL1 and TM3 hydrophobically and with ECL3 through polar interactions **(**Fig. 2B**)**.

The dimer interface at the 7TM domain can be separated into two parts. The first is formed at the extracellular end by TM4, TM5 and ECL2 of each protomer. The helices assemble in an inverted V-shape, creating a cavity. The second interaction at the cytoplasmic end closes the cavity. (Fig. 2C and fig. S6C). This type of dimeric architecture has not been seen in other GPCRs, including class C receptors. (fig. S6D).

The extracellular portion of the TM interface formed by TM4, TM5, and ECL2 features a series of hydrophilic interactions and hydrophobic contacts (Fig. 2C). The cytoplasmic portion of the TM interface is formed by TM3 and ICL2 of both the protomers. The ICL2 regions interact with each other and residues in TM3 form a basic patch that engages phospholipids (fig. S6, C and E). The polar contacts between Q516 across protomers also form the lid that covers the cavity from the intracellular end (II in Fig. 2C). The cavity formed at the dimer interface is further shielded at both intra- and extracellular ends by several cholesterol molecules from both the front and back sides (fig. S6A). The TM domain interaction with cholesterols may stabilize the dimeric interface.

We observed densities for two phospholipids at the cavity formed by the TM dimeric interface and performed mass-spectrometry to identify lipids co-purified with GPR158 complex (fig. S6F). Although not exhaustive, this lipidomics analysis identified several phospholipid species, most notably Phosphatidylethanolamine (PE) and Phosphatidylinositol (PI). Both molecules are well accommodated into the respective cryoEM densities (Fig. 2A and fig. S3). The phospholipids are arranged in the cavity in such a way that one hydrophobic tail of each lipid is inserted into the shallow hydrophobic pocket created by TM3, TM4 and TM5 stabilizing the dimer interface. The hydrophobic tails of PE and PI are

stacked against the side chains of bulky hydrophobic residues, and head groups occupy basic clusters at the interface. (fig. S6, G and H). Comparisons with other class C GPCR structures show both similarities and differences in 7TM organization (fig. S7).

Overall, the distinct dimeric arrangement of the TM domain that forms an extensive web of interactions, and the additional stability conferred by phospholipids and cholesterol molecules interactions make the TM dimeric interface more compact and unlikely to be compatible with G protein activation. Indeed, our functional studies of GPR158 show no constitutive activity in any of the G protein signaling assays (fig. S8). Furthermore, mutagenesis at the dimerization interface aimed at increasing the dynamics by mimicking substitutions that activate other class C GPCRs (20),(21) also failed to unlock the constitutive activity of GPR158 (fig. S8 and table S2). We conclude that the GPR158 7TM domain has an organization of the dimeric interface that locks it in a conformation that prevents constitutive G protein activation.

The ECDs of two protomers interact with each other side-by-side forming cross-subunit contacts. The ectodomain of each protomer is composed of the N-terminal α-helical region, a prominently folded central domain, and a C-terminal stalk region (Fig. 3A). Superposition of the two ECDs showed substantial structural similarity with an r.m.s.d. of 1.37 Å **(**fig. S9A**)**. The largest portion of the GPR158 ectodomain comprising 412 amino acids lacks sequence similarity with ectodomains of other GPCRs. The GPR158 structure reveals a well-defined globular domain consisting of six antiparallel β-sheets flanked by two α-helices (Fig. 3B). A structural homology search revealed that it shares a similar fold to Cache (CAlcium channels and CHEmotaxis receptors) domains present in numerous proteins but not previously found in GPCRs. The β-sheets of the Cache domain are curved and form an amphipathic pocket analogous to a ligand-binding site in the Cache domains of other proteins (Fig. 3C). The helices α1 and α2 assemble at the back of β-sheets core structure, stabilizing the cavity by hydrophobic interactions with β-sheets residues. The density for third helix, α3 at respective position is not well resolved to correctly interpret. The α3 likely capping the putative ligand-binding pocket from one side while being connected by flexible loops (β3α3 and α3β4) (Fig. 3B). The density surrounding the binding pocket is not uniformly resolved, likely reflecting its dynamic nature. It possibly becomes ordered upon ligand binding. The Cache domain of GPR158 has the highest structural homology with the ligand sensing extracellular Cache domains of the bacterial chemoreceptors and Histidine kinase receptors **(**fig. S9B**)**.

The Cache domain is connected via NTD-Cache loop to the N-terminal domain (NTD) which has three helices. The NTD-Cache loop contains C99 that forms a disulfide bond with C272 of the Cache domain β4β5 loop. Interactions with the NTD-Cache loop and N-terminal region likely provide additional stability to the Cache domain.**(**fig. S9C**)**. The C-terminus of the Cache domain is connected to the stalk region that contains flexible loops and has very weak density map. The stalk region is cysteine-rich, and its ten cysteines may engage in intradomain disulfide bridges **(**fig. S9D**)**. A structurally similar cysteine-rich domain (CRD) is found in class C GPCR suggesting that it likely plays a similar role in receptor activation (21, 22). Following the stalk region is a stalk-TM linker that hydrophobically interacts with ECL2 and connects to TM1 of the transmembrane domain.

One of the most prominent features of the GPR158 ectodomain is the dimerization of the Cache domains which occurs through helices α1 and α2 of each Cache domain which cross at an angle to create a four-helix bundle at the dimer-interface (fig. S9E). The loops connecting helices α1 and α2 are also likely involved in inter-subunit interaction. The dimer interface is stabilized by an extensive network of hydrophobic and hydrophilic interactions, with a buried surface area of 2178.3 $Å^2$ (fig. S9F).

The structure of the GPR158 homodimer bound to the RGS7-Gβ5 complex revealed several key insights into the RGS docking and regulation by GPCRs. Overall, we observed an asymmetric assembly involving two GPR158 protomers interacting with one RGS7-Gβ5 complex (Fig. 1B). The two docking sites for RGS7-Gβ5 on GPR158 are both created by the dimerization of GPR158. Upon RGS7 binding to GPR158, the intracellular C-terminal helices of both GPR158 protomers, which were disordered in the GPR158-apo structure, stack into a coiled-coil configuration (CT-CC). The side chain densities are not well resolved for CT-CC residues and have high B-factor (fig. S4D). The CT-CC domain contributes a third contact point for the dimerization of GPR158 in the complex predicted to be held together mainly by hydrophobic contacts and stabilized by ionic and polar bonding (fig. S10, A to E). The contacts with GPR158 are made exclusively by RGS7 with no direct interactions involving Gβ5.

The primary binding site (site I) is formed by CT-CC (Fig. 4A) that potentially engages in an extensive web of hydrophobic and hydrophilic interactions with the RGS7 DEP-DHEX domain (fig. S10, F to H). One α-helix is engaged in the interactions with Eα1, Eα3, and Eα4 helices; Eα3Eα4 and DEP-DHEX loops, whereas the other α-helix interacts with Eα3 helix, Eα2Eα3, and DEP-DHEX loops. In addition, we observe insertion of the C-terminal loop in one of the GPR158 protomers with the pocket created by DEP Dα1 and DHEX Eα4 helices, and β-hairpin loop (fig. S10H). The second docking site (site II) for RGS7-Gβ5 is provided by the intracellular portion of the 7TM dimerization interface. However, the contacts at this site are made only with one GPR158 protomer. The interaction involves TM3, TM5, and ICL3 of GPR158 7TM domain and Eα1, Eα2, Eα3 helices and Eα1Eα2 loop of DHEX domain (Fig. 4A). The interactions at this interface are mainly hydrophobic stabilized by hydrogen bonding at the periphery (fig. S10I). Comparison with the apo structure shows that RGS7-Gβ5 binding results in pulling the GPR158 protomers apart remodeling the interface to accommodate RGS7 (Fig. 4B).

The GPR158-RGS7 interactions at the second site are weaker than the binding to CT-CC, likely transient in nature, and involve remodeling of both GPR158 and RGS7-Gβ5. Comparison of the apo GPR158 structure with the structure of the GPR158-RGS7-Gβ5 complex reveals re-arrangement of the cytoplasmic end of TM3 and ICL2 of one 7TM, shifting inward towards its 7TM core upon RGS7 binding. This is accompanied by destabilization of the TM3 C-terminus and ICL2 at the other 7TM protomer affecting the 7TM dimerization interface (Fig. 4B). Comparison of the apo RGS7-Gβ5 crystal structure (23) with the complex structure also shows substantial re-organization of the RGS7 DEP-DHEX domain upon binding to GPR158 (Fig. 4C). Most prominently, the dynamic loop Eα1Eα2 moves upward and is stabilized by interacting with TM3, TM5 and ICL3. Along with this, DHEX helices Eα1, Eα2, and Eα3 moved upward to interact with the TM domain

and the DEP-DHEX loops move upward to interact with GPR158 CT. The β-hairpin loop of RGS7 moves upward so that its hydrophobic tip is inserted into the membrane allowing Dα2 helix rearrangement in the DEP domain (Fig. 4B). These rearrangements collectively generate favorable complementary electrostatic surfaces on the GPR158-RGS7 interface. This likely serves to orient RGS7-Gβ5 complex toward the membrane (fig. S10, J and K).

RGS7 recruitment is reminiscent of GPCR interactions with signal transducers. Indeed, the RGS binding surface on GPR158 substantially overlaps with the GPCR surface that binds heterotrimeric G proteins and β-arrestin (fig. S11, A and B). Our modeling using structures of Gα complexes with diverse GPCRs shows that the RGS7 DHEX domain occludes the G protein binding site from the TM3 and TM5 side where the α5 helix of Gα inserts into 7TM central cavity and creates steric clashes with the Ras domain of Gα subunits (fig. S11, C to E). Thus, recruitment of RGS7-Gβ5 would preclude GPR158 from productively interacting with G proteins, supporting lack of G protein activation (fig. S8). We further detect bidirectional allosteric effects resulting from the GPR158-RGS7 binding similar to what is observed upon GPCR-Gα interaction. These include inward shift of the cytoplasmic end of TM3, as seen in the $GABA_B$-Gi structure and modulation of the ligand-binding ectodomain upon RGS7 binding. The interaction of GPR158 with RGS7-Gβ5 complex is quite distinct and mutagenesis at the GPR158 dimerization interface that constutitvely activate class C GPCRs failed to change RGS activity in the absence of a ligand (fig. S12).

To further investigate conformational dynamics resulting from RGS7-Gβ5 recruitment to GPR158 we performed biochemical experiments. First, we studied the impact of binding to a synthetic C-terminal peptide that comprises the CT-CC module by gel filtration. Complexing with this peptide was sufficient to induce a large change in hydrodynamic behavior of the RGS7-Gβ5 complex consistent with substantial conformational changes in RGS7-Gβ5 upon binding to GPR158 (fig. S13A). We further refined these investigations using HDX-MS which showed that the C-terminal peptide induced significant changes in solvent accessibility within the DEP-DHEX domain, specifically in Dα1, Eα3 and Eα4 helices, β-hairpin, Eα3Eα4 and DEP-DHEX loops of RGS7 (fig. S13, B to D).

In this work, we present high-resolution structures of an unusual receptor assembly that involves an orphan GPCR complexed with a signaling regulator- RGS protein. The RGS protein binds the same elements that GPCRs use for engaging their signal transducers: G proteins and β-arrestins. In the present structure we observe constitutive engagement of RGS7/Gβ5 complex by GPR158 in the absence of a G protein. We speculate that binding of a ligand to the extracellular ECD would activate GPR158 rearranging of the cytoplasmic domains that engage RGS to alter its activity. Given that RGS binding precludes GPR158 from canonical activation of G proteins, one can describe it as an RGS-coupled receptor.

In addition to providing information on the GPCR-RGS structure we show the role of two phospholipids in organizing the dimerization interface of GPCRs. These lipids staple the protomers and provide intriguing possibilities for GPCR modulation. We also identify a Cache domain raising the possibility that GPR158 detects a small molecule ligand that could regulate of the RGS module, an avenue to be explored in future studies. In conclusion, we hope our findings will spur further progress in understading the regulatory and signaling

mechanisms of GPR158 by facilitating the structure-based discovery of its ligands and by guiding exploration of GPR158-mediated control of RGS proteins in the endogenous neuronal setting.

Supplementary Material

Refer to Web version on PubMed Central for supplementary material.

ACKNOWLEDGEMENTS

We are indebted to our colleagues at The Scripps Research Institute, Drs. Erumbi S. Rangarajan and Marina Candido Primi, for their daily help throughout the project which led to the generation of homogeneous samples required for high-resolution cryoEM single-particle analyses as well as generous and unlimited access to their dedicated equipment that was necessary to obtain the cryoEM structure reported here. We thank the staffs Adam Wier, Thomas Edwards and Ulrich Baxa of the NCI National CryoEM Facility for data collection. We also thank Dabbu Kumar Jaijyan for help with cryo-EM sample.

Funding:

This work was supported by NIH grants MH105482 (to K.A.M.) and GM127883 (to J.F.H.). This research was, in part, supported by the National Cancer Institute's National CryoEM Facility at the Frederick National Laboratory for Cancer Research under contract HSSN261200800001E. AKS is a IYBA and Ramalingaswamy DBT fellow and is supported by SERB-SRG funding agency (SERB/SRG/2020/000266). This research was funded in whole, or in part, by the Wellcome Trust Grant No. 104633/Z/14/Z. For the purpose of Open Access, the author has applied a CC BY public copyright license to any Author Accepted Manuscript version arising from this submission. During the course of this project, TI was supported by grants from the Department of Defense, the National Science Foundation, The National Institutes of Health, and by start-up funds provided to the Scripps Research Institute from the State of Florida.

Data availability:

The cryoEM density maps and Coordinates have been deposited in the Electron Microscopy Data bank (EMDB) and Protein Data Bank (PDB), respectively, with accession codes MD-25125 and 7SHE for GPR158 apo; and EMD-25126 and 7SHF for GPR158-RGS7/Gβ5 Complex. The crosslinking mass spectrometry proteomics data have been deposited to the ProteomeXchange Consortium via the PRIDE (24) partner repository with the dataset identifier PXD026603. *Submission details: Project Name:* XL-MS Analysis of Recombinant GPR158-RGS7-Gβ5 Complex in Detergent Micelles, *Project accession:* PXD026603, *Project DOI*: Not applicable, *Reviewer account details: Username:* reviewer_pxd026603@ebi.ac.uk, *Password:* euMtHAf4 Raw HDX-MS data are deposited at https://figshare.com/s/56c03387d510fd39eb08. Raw lipidomics data are deposited at https://figshare.com/s/f78c92eca1f90fe485d3.

References and notes

1. Hauser AS et al. Pharmacogenomics of GPCR Drug Targets. Cell 172, 41–54 e19 (2018). [PubMed: 29249361]
2. Sriram K, Insel PA, G Protein-Coupled Receptors as Targets for Approved Drugs: How Many Targets and How Many Drugs? Mol Pharmacol 93, 251–258 (2018). [PubMed: 29298813]
3. Gilman AG, G proteins: transducers of receptor-generated signals. Annu Rev Biochem 56, 615–649 (1987). [PubMed: 3113327]
4. Shukla AK, Xiao K, Lefkowitz RJ, Emerging paradigms of beta-arrestin-dependent seven transmembrane receptor signaling. Trends Biochem Sci 36, 457–469 (2011). [PubMed: 21764321]

5. Hollinger S, Hepler JR, Cellular regulation of RGS proteins: modulators and integrators of G protein signaling. Pharmacol Rev 54, 527–559 (2002). [PubMed: 12223533]
6. Ross EM, Wilkie TM, GTPase-activating proteins for heterotrimeric G proteins: regulators of G protein signaling (RGS) and RGS-like proteins. Annu Rev Biochem 69, 795–827 (2000). [PubMed: 10966476]
7. Abramow-Newerly M, Roy AA, Nunn C, Chidiac P, RGS proteins have a signalling complex: interactions between RGS proteins and GPCRs, effectors, and auxiliary proteins. Cell Signal 18, 579–591 (2006). [PubMed: 16226429]
8. Ballon DR et al. DEP-domain-mediated regulation of GPCR signaling responses. Cell 126, 1079–1093 (2006). [PubMed: 16990133]
9. Civelli O, Orphan GPCRs and neuromodulation. Neuron 76, 12–21 (2012). [PubMed: 23040803]
10. Insel PA et al. G Protein-Coupled Receptor (GPCR) Expression in Native Cells: "Novel" endoGPCRs as Physiologic Regulators and Therapeutic Targets. Mol Pharmacol 88, 181–187 (2015). [PubMed: 25737495]
11. Orlandi C et al. GPR158/179 regulate G protein signaling by controlling localization and activity of the RGS7 complexes. J Cell Biol 197, 711–719 (2012). [PubMed: 22689652]
12. Patel N et al. Expression and functional role of orphan receptor GPR158 in prostate cancer growth and progression. PLoS One 10, e0117758 (2015). [PubMed: 25693195]
13. Khrimian L et al. Gpr158 mediates osteocalcin's regulation of cognition. J Exp Med 214, 2859–2873 (2017). [PubMed: 28851741]
14. Sutton LP et al. Orphan receptor GPR158 controls stress-induced depression. eLife 7, (2018).
15. Engqvist H et al. Immunohistochemical validation of COL3A1, GPR158 and PITHD1 as prognostic biomarkers in early-stage ovarian carcinomas. BMC Cancer 19, 928 (2019). [PubMed: 31533654]
16. Condomitti G et al. An Input-Specific Orphan Receptor GPR158-HSPG Interaction Organizes Hippocampal Mossy Fiber-CA3 Synapses. Neuron 100, 201–215 e209 (2018). [PubMed: 30290982]
17. Song C, Orlandi C, Sutton LP, Martemyanov KA, The signaling proteins GPR158 and RGS7 modulate excitability of L2/3 pyramidal neurons and control A-type potassium channel in the prelimbic cortex. J Biol Chem 294, 13145–13157 (2019). [PubMed: 31311860]
18. Orlandi C et al. Orphan Receptor GPR158 Is an Allosteric Modulator of RGS7 Catalytic Activity with an Essential Role in Dictating Its Expression and Localization in the Brain. J Biol Chem 290, 13622–13639 (2015). [PubMed: 25792749]
19. Orlandi C, Sutton LP, Muntean BS, Song C, Martemyanov KA, Homeostatic cAMP regulation by the RGS7 complex controls depression-related behaviors. Neuropsychopharmacology 44, 642–653 (2019). [PubMed: 30546127]
20. Park J et al. Structure of human GABAB receptor in an inactive state. Nature 584, 304–309 (2020). [PubMed: 32581365]
21. Koehl A et al. Structural insights into the activation of metabotropic glutamate receptors. Nature 566, 79–84 (2019). [PubMed: 30675062]
22. Du J et al. Structures of human mGlu2 and mGlu7 homo- and heterodimers. Nature 594, 589–593 (2021). [PubMed: 34135509]
23. Patil DN et al. Structural organization of a major neuronal G protein regulator, the RGS7-Gbeta5-R7BP complex. eLife 7, (2018).
24. Perez-Riverol Y et al. The PRIDE database and related tools and resources in 2019: improving support for quantification data. Nucleic Acids Res 47, D442–D450 (2019). [PubMed: 30395289]

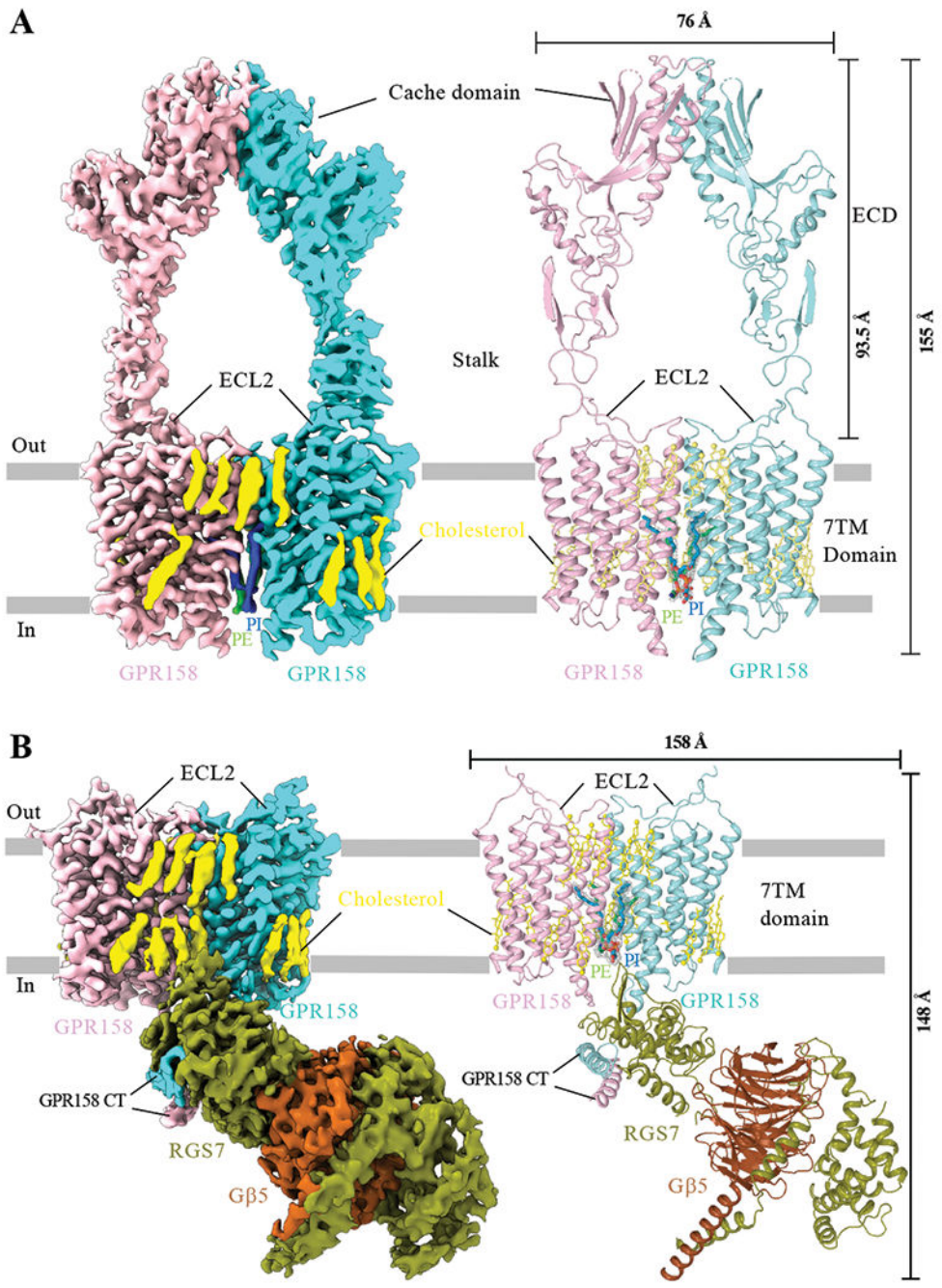

Fig. 1. CryoEM structures of GPR158 in its apo and RGS7-Gβ5 bound states.

(**A**) CryoEM map (left) and model (right) of GPR158 homodimer in ribbon representation with protomers colored in cyan and pink. Phospholipids PE and PI, and cholesterols are shown in green, blue, and yellow colors, respectively. (**B**) CryoEM map (left) and model (right) of GPR158 homodimer complexed with RGS7-Gβ5 in ribbon representation colored as (**A**) and RGS7 and Gβ5 are shown in deep-olive and brown color.

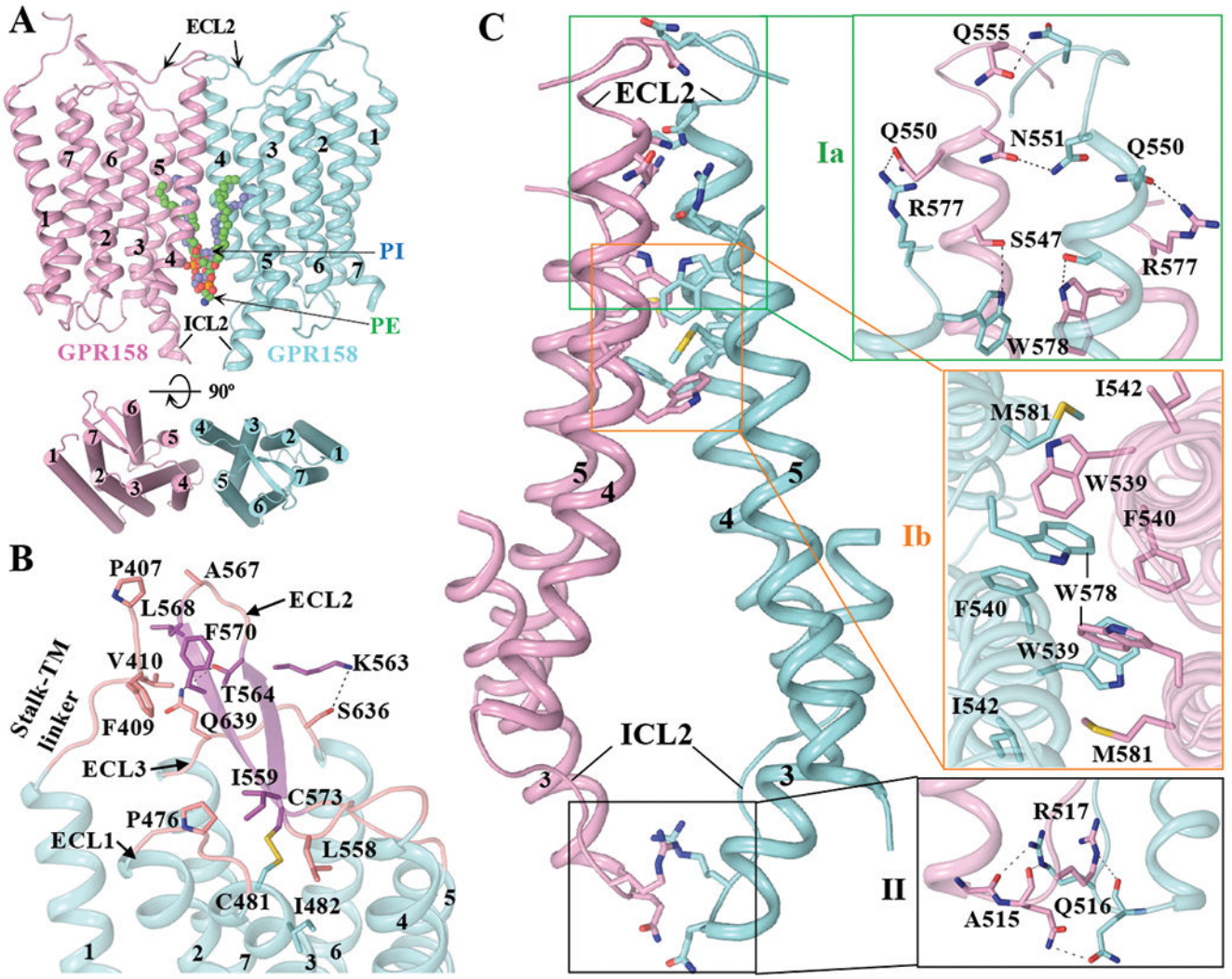

Fig. 2. Organization of GPR158 transmembrane domain and its homodimer interface.

(**A**) Overall arrangement of the 7TM region of GPR158 protomers is shown as side and top view. Phospholipids PE and PI are identified at the cavity formed by TM dimeric interface are shown in spheres representation. 7TM protomers and phospholipids are colored as Fig.1. (**B**) Close-up view of the extracellular loop region. ECL2 caps the extracellular pocket by interacting with TM3, ECL1, and ECL3 residues. ECL2 C573 preserves the conserved disulfide bond with TM3 C481. ECL2 is also stabilized by interaction with a stalk-TM linker that connects ectodomain with 7TM. (**C**) The 7TM dimer interface is formed at two sites (I and II), the extra- and intracellular side. Direct contacts at the extracellular side are formed by TM4, TM5, and ECL2 of both protomers, and contacts are shown in the right panels. Intracellular side interface is formed by TM3 and ICL2 of both protomers and contacts formed by ICL2 are shown in the right panel.

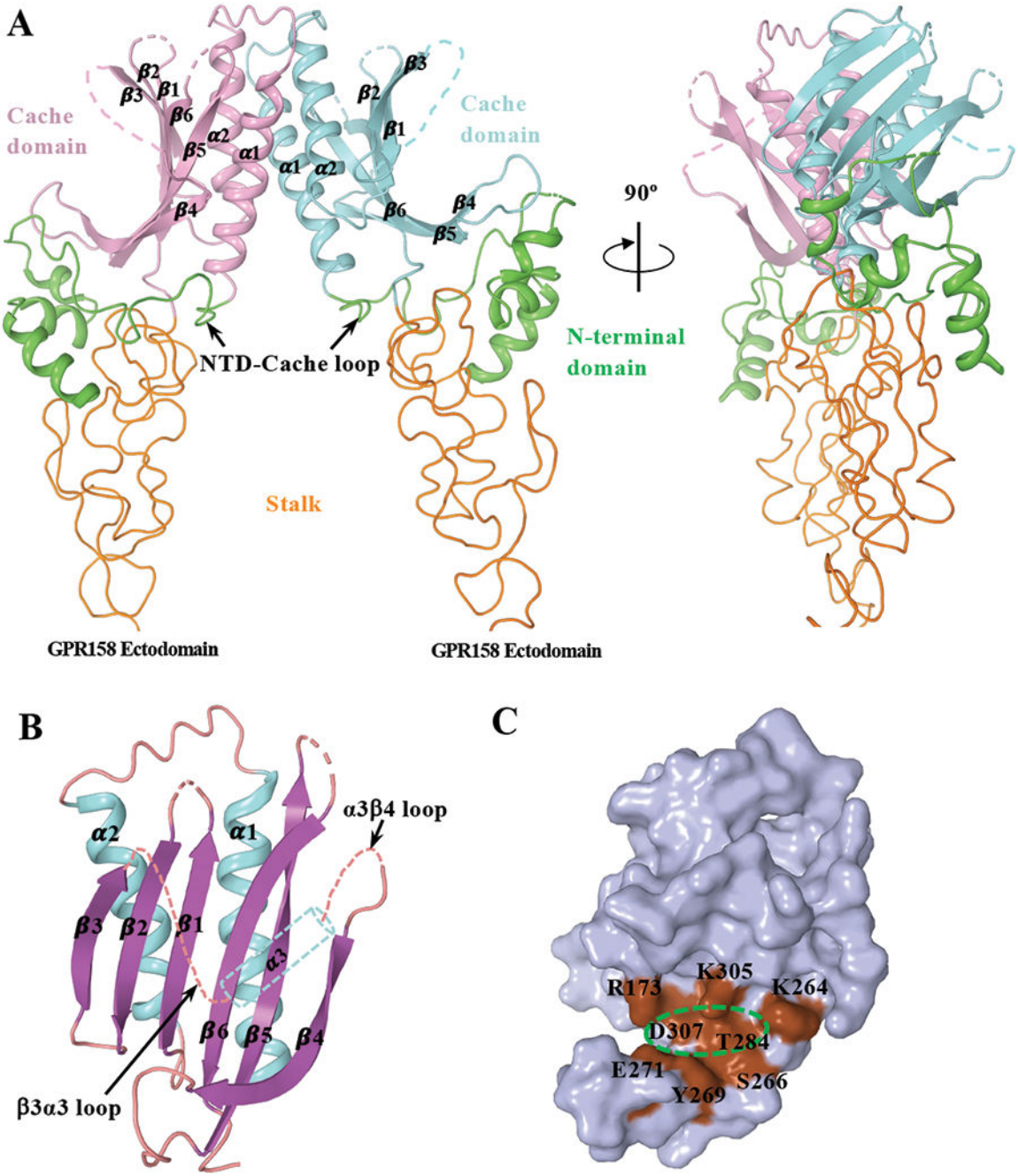

Figure 3. A unique organization of the GPR158 ectodomain featuring the Cache domain.

(**A**) Side view of GPR158 ectodomain consisting of N-terminal domain (NTD), Cache domain, and stalk region. The GPR158 ectodomain forms a dimeric interface with the Cache domain. (**B**) The Cache domain is composed of six antiparallel β-sheets flanked by α-helices. The density for α3 helix is not well resolved and is represented as dotted cylinder at respective position. The missing flexible loops in the model are shown in dotted lines. (**C**) Cache domain putative ligand-binding pocket. The curved sheets form a putative ligand-binding pocket (dotted oval), equivalent to the prokaryotes extracellular Cache domain

ligand binding site, generates an amphipathic environment. The putative ligand interacting residues shown in brown color. However, densities for the most side chains of pocket residues are not well resolved and have high B-factor. The putative ligand binding pocket is possibly capped by dynamic α3 helix from one side.

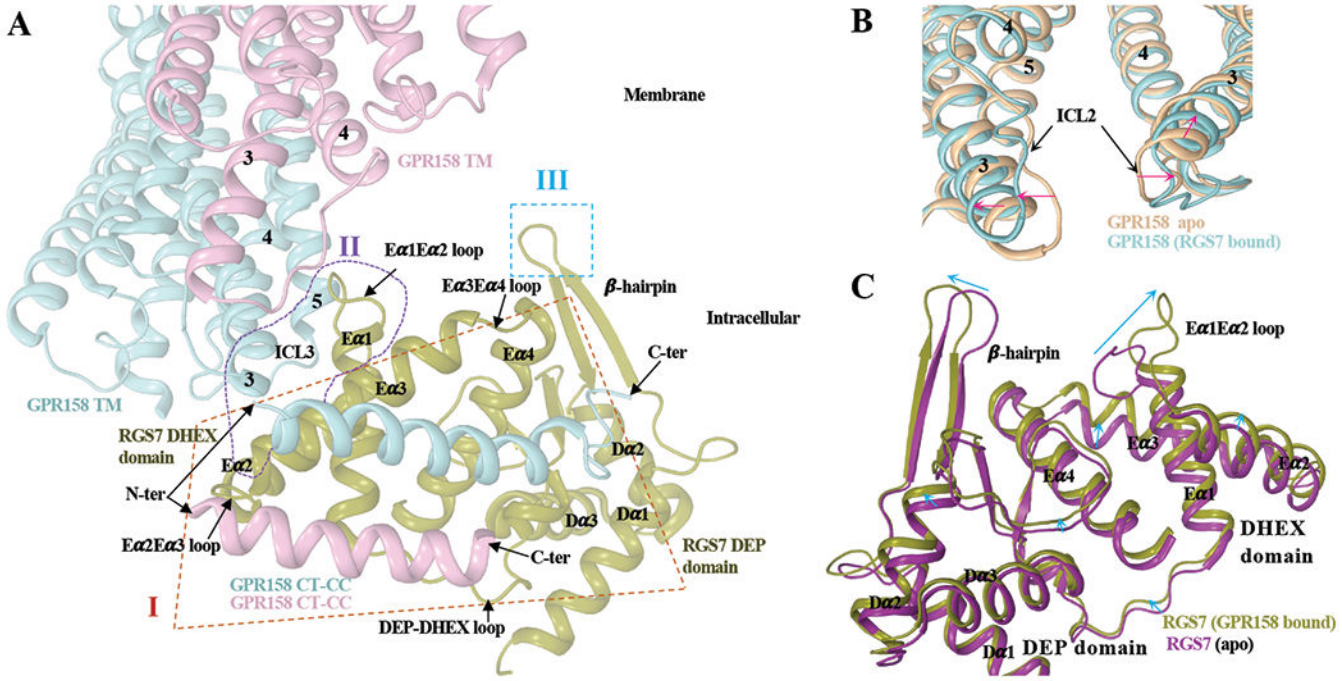

Figure 4. Mechanism of GPR158 interaction with RGS7.

(**A**) RGS7 forms two distinct binding sites (I and II) on GPR158, both created by the dimerization of GPR158. The first binding interface is formed between GPR158 CT-CC and RGS7 DEP-DHEX domain. The second interface is formed by GPR158 7TM and RGS7 DHEX domain. In addition, β-hairpin loop of RGS7 is inserted into the membrane (shown as III) and could facilitate the orientation of RGS7 towards the membrane. (**B and C**) Conformational rearrangement on GPR158 TM dimeric interface and RGS7 upon complex formation. The TM3 of one protomer shifts toward the 7TM core while dissociating it from another protomer to accommodate RGS7 at the interface (**B**). Large conformation shift at Eα1Eα2 loop of RGS7 DHEX domain along with rearrangement of β-hairpin loop and helices that shifted up towards the membrane (**C**).